Journal of Materials Chemistry A

Accepted Manuscript

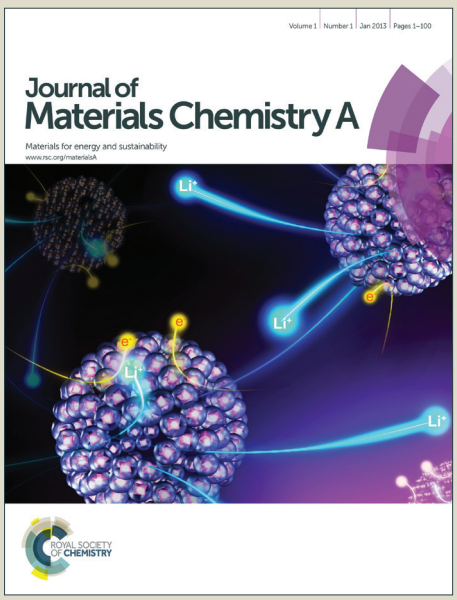

ROYAL SOCIETY OF CHEMISTRY

www.rsc.org/materialsA

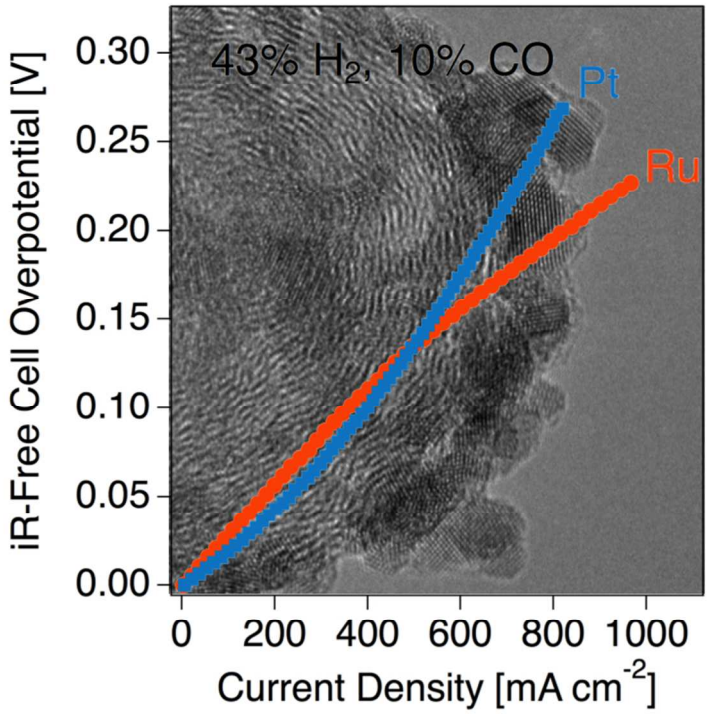

In solid acid fuel cells operating at 250 C, Ru catalysts are more tolerant to CO than Pt.

Ruthenium as a CO-Tolerant Hydrogen Oxidation Catalyst for Solid Acid Fuel Cells†

Alexander B. Papandrew,*[a] Robert W. Atkinson III,[a] Raymond R. Unocic,[b] and Thomas A. Zawodzinski, Jr.[a,c]

Received Xth XXXXXXXXXX 20XX, Accepted Xth XXXXXXXXX 20XX
First published on the web Xth XXXXXXXXXX 200X
DOI: 10.1039/b000000x

Carbon supported Ru nanoparticles were implemented in composite anodes of fuel-generating hydrogen pumps and electricity-generating fuel cells based on the inorganic proton conductor CsH_2PO_4. In cells operating at 250 °C, Ru catalysts are more tolerant to CO than Pt at cell currents greater than 500 mA cm^{-2} and are stable in a fuel stream containing 10% CO for over 160 hours. Hydrogen-air fuel cells fabricated with Ru-based anodes performed comparably to those with Pt-based anodes in both pure hydrogen and in a hydrogen-rich simulated reformate containing 10% CO.

1 Introduction

Fuel cells operating on hydrogen have been proposed as efficient alternatives to combustion-based energy conversion technologies for automotive and stationary applications. In the case of low-temperature fuel cells, a high-purity hydrogen stream is required to avoid adsorptive poisoning by impurities of the metal anode catalyst, which is typically Pt. This restriction may represent a barrier to adoption of these technologies, since in the absence of a hydrogen generation scheme based on renewables, hydrogen is overwhelmingly derived via steam reforming of hydrocarbons. That hydrogen must be separated from the undesired components in the reformate stream, with a net result of increased hydrogen cost. Technologies operating at elevated temperatures mitigate the impact of fuel impurities. One such promising system is based on the crystalline inorganic proton conductor CsH_2PO_4 [1] (CDP) and typically operates at 250 °C. A disadvantage of CDP-based electrochemical systems is the use of Pt in device electrodes with loadings from 0.4 to 1.0 mg_{Pt} cm^{-2} on the anode [2] and greater than 1.5 mg_{Pt} cm^{-2} on the cathode [3]. Recently, we showed that Pd can be substituted for Pt in anodes [2], potentially enabling more economical electrode formulations. In this communication, we show that Ru is also suitable as an anode catalyst, and in fact is superior to Pt at high cell currents in CO-rich fuel streams.

Ruthenium is well-known as a crucial alloying element (with Pt) in catalysts for methanol electrooxidation [4,5], due to its synergistic effects on CO removal from Pt. It is significantly less useful for the hydrogen oxidation reaction (HOR) in low-temperature acidic environments, with a typical activity 2 to 3 orders of magnitude lower than Pt [6]. Recent work has shown that a different scenario may exist in low-temperature alkaline media, where Ru displayed size-dependent activity for the HOR that can exceed Pt for certain particle sizes [7,8]. Reports of elemental Ru HOR catalysts at intermediate temperatures (100-300 °C) are few, but a recent investigation has appeared discussing applications of Ru in H_2-air cells based on Sb-doped tin pyrophosphate membranes [9].

Supported Ru catalysts are typically prepared by established methods [10,11] such as solution-phase reduction or impregnation and calcination. Here, we have opted for a vapor-phase route to carbon-supported Ru to obtain the high metal loadings and conformal support decoration previously established to be required for acceptable SAFC electrode performance [2,3,12]. While chemical vapor deposition methods have been used to deposit Ru [13–15] and Ru-alloy [16] thin films for some time, these methods require specialized apparatus to effect the synthesis of highly dispersed supported nanoparticles [17,18]. Recently, we showed that supported Pt [2,3], Pd [2], and Pt-Pd alloy [12] nanoparticulate catalysts can be synthesized on diverse supports using a single-step fixed-bed procedure at low temperature (approximately 200 °C) with no special apparatus using acetylacetonate (acac) precursors. We conjectured that this method could be extended to the synthesis of Ru, given the adsorption [19] and thermolysis [19,20] characteristics of $Ru(acac)_3$ and related [21] Ru β-diketonates.

[a] *Chemical and Biomolecular Engineering, University of Tennessee, Knoxville, TN, USA. Fax: (865) 974-7076; Tel: (865) 974-2421; E-mail: apapandrew@utk.edu*
[b] *Center for Nanophase Materials Sciences, Oak Ridge National Laboratory, Oak Ridge, TN, USA.*
[c] *Materials Science and Technology Division, Oak Ridge National Laboratory, Oak Ridge, TN, USA.*

2 Experimental

The supported Ru catalyst (60 wt%) was synthesized on Vulcan XC-72R support in a fixed bed in a N_2-water vapor atmosphere. Solid $Ru(acac)_3$ precursor (Sigma-Aldrich) was mechanically mixed with as-received Vulcan XC-72R (Cabot Corp.) in a glass vial. The vial was placed in a vacuum oven along with a separate vessel containing 2.3 mL of deionized liquid water. The oven was subsequently evacuated with a rotary vane vacuum pump and purged with dry N_2 several times, and finally evacuated again to 0.30 bar and heated to 240 °C. During the thermal treatment, the liquid water vaporized, the $Ru(acac)_3$ precursor sublimed, and Ru^0 was deposited on the support. After 15 h at 240 °C, the oven was cooled to room temperature. The final weight of the carbon supported catalyst was consistent with complete decomposition of the $Ru(acac)_3$ complex to Ru metal.The carbon-supported catalysts were characterized with monochromatic Cu Kα x-ray diffraction (XRD) (Philips X'Pert, λ=0.1541874 nm) and transmission electron microscopy (Hitachi HF-3300 TEM/STEM operating at 300 kV). A control sample of 60wt%Pt/C was synthesized via a similar method, as detailed previously[2].

Composite electrocatalyst powders were synthesized by dry-grinding CDP, the experimental 60wt%Ru/C catalyst (or 60wt%Pt/C in the case of the control sample), and naphthalene (as a fugitive binder) in a 3:1:1 ratio by weight. Both air-breathing hydrogen fuel cells and electrochemical hydrogen pumps were then fabricated using these electrocatalysts. Membrane-electrode assemblies (MEAs) were fabricated by lamination of active layers in a 0.75 (2.85 cm^2) in diameter hardened steel die. Stainless steel mesh (grade 304) was used for current collectors, and expanded PTFE tape was used for sealing. Each MEA had a CDP membrane thickness of approximately 50 to 60 μm. In the case of the air-breathing cells, the anode was comprised of 25 mg of the composite electrocatalyst (either Pt or Ru with a metal loading of 1.0 mg cm^{-2}) laminated at 125 MPa, while the cathode consisted of vapor-deposited Pt:CDP[3] with a loading of 1.75 mg_{Pt} cm^{-2} laminated at 8 MPa. Hydrogen pumps were either Pt-Pt symmetrical control cells with 1.0 mg_{Pt} cm^{-2} on each electrode, or cells for which one of these electrodes is replaced with 25 mg of the Ru-based electrocatalyst (1.0 mg_{Ru} cm^{-2}). All hydrogen pump electrodes were laminated at 125 MPa. Hydrogen electrodes were grossly similar irrespective of the use of Pt or Ru catalysts and strongly resemble those observed in our earlier work[2]. Electrolyte particles of approximately 1 μm in diameter were used for all electrodes.

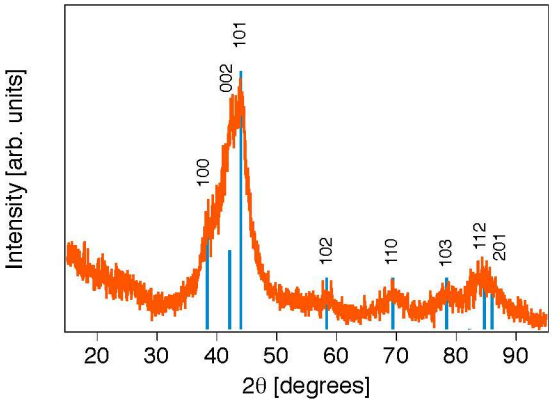

Fig. 1 Cu Kα x-ray diffraction patterns for vapor-grown 60%Ru /XC72 (trace) and indexed peak positions with relative intensities (sticks) for Ru metal (PDF 00-006-0663).

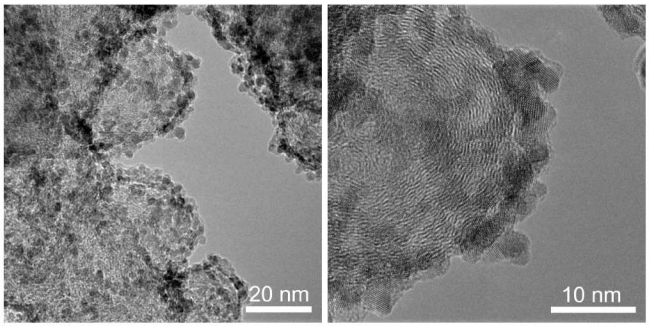

Fig. 2 High resolution transmission electron micrographs of the Ru nanoparticles dispersed on a Vulcan XC-72R support from a vapor phase $Ru(acac)_3$ precursor.

Electrochemical cell testing was conducted at 250 °C with gases hydrated to a dew point of 73 °C to 75 °C (approximately 0.35 bar water partial pressure). Anodes were supplied either ultrahigh purity H_2 or simulated propane reformate with a composition of 43% H_2, 37% N_2, 10% CO, 9.75% CO_2, 0.25% CH_4. All hydrogen pump cathodes were supplied ultrahigh purity H_2; all H_2-air cathodes were supplied ultrahigh-purity air. Polarization curves were recorded with a Bio-Logic VSP potentiostat by scanning the working electrode potential at 5 mV s^{-1} from the open circuit potential to an arbitrary cell potential (0.5 V for H_2 pumps, 0.2 V for H_2-air cells). Potentiostatic electrochemical impedance spectroscopy (EIS) spectra were recorded from 200 kHz to 200 mHz at selected potentials with single sine perturbation amplitude of 10 mV. The high-frequency intercept of the EIS spectrum was used to eliminate the ohmic resistance of the CDP membrane from the polarization curves, yielding what we hereafter refer to as iR_Ω-free polarization curves. Raw polarization curves absent of this correction are shown in the ESI.

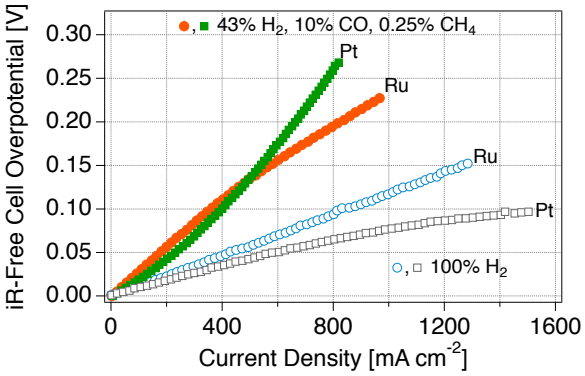

Fig. 3 iR_Ω-free hydrogen oxidation polarization curves for hydrogen pumps with Pt-based or Ru-based composite anodes and Pt-based cathodes acquired at 250 °C and 75 °C dew point in 100% H_2 (open markers) and in a simulated reformate mixture (43%H_2, 37% N_2, 10% CO, 9.75% CO_2, 0.25% CH_4) (filled markers).

3 Results and Discussion

The XRD pattern (Figure 1) of the as-synthesized supported Ru shows size-broadened peaks characteristic of hexagonal Ru metal. Scherrer analysis of the pattern using the Philips X'Pert Highscore software returned a mean crystalline domain size of 3.5 nm. This particle size estimate is supported by TEM (Figure 2), which additionally shows that the catalyst consists of a high metal loading of nanometer-scaled Ru particles coating the carbon support conformally. All of the metal observed was present in contact with the carbon support. X-ray absorption measurements indicate the presence of surface oxide and confirm interatomic spacings consistent with an Ru metal standard (see ESI).

In an electrochemical hydrogen pump, molecular hydrogen is oxidized at an anode, protons are "pumped" across the CDP membrane by an applied potential, and molecular hydrogen is evolved at the cathode. Devices based on this concept can be used to produce purified hydrogen from multicomponent gas streams[2,22,23]. In CDP-based systems, this configuration is also valuable for evaluating the activity and impurity tolerance of HOR catalysts by eliminating the large overpotentials associated with oxygen reduction at the cathode of an H_2-air cell. Figure 3 shows the performance of hydrogen pumps with Pt- and Ru-based anodes in hydrogen and in the hydrogen-containing reformate mixture. In hydrogen, the Pt anode is marginally superior to the Ru anode as evinced by the lower cell overpotentials required at any current density. In the CO-rich gas mixture, however, the situation is more complex. At current densities less than 500 mA cm^{-2}, the Pt anode is still slightly more active than the Ru anode, but the disparity in overpotential is smaller (approximately 14 mV). Beyond 500 mA cm^{-2}, the polarization curves cross, and the Ru anode becomes the more active electrode.

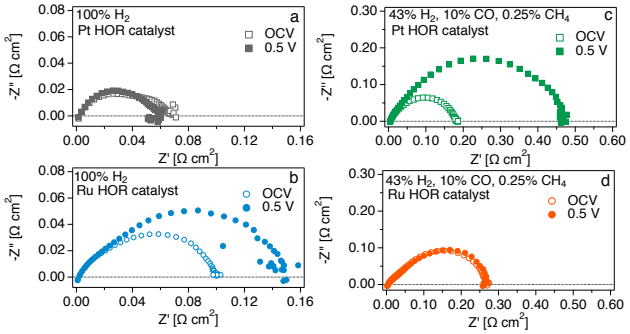

Fig. 4 iR_Ω-free hydrogen EIS spectra for hydrogen pumps at OCV and 0.5 V cell potential in 100% H_2 and in simulated reformate (see text for full composition) **(a)** Pt anode, 100% H_2 **(b)** Ru anode, 100% H_2 **(c)** Pt anode, simulated reformate **(d)** Ru anode, simulated reformate

Figure 4 shows Nyquist plots acquired at the open circuit voltage (OCV) and at a cell voltage of 0.5 V for each of the electrodes and conditions shown in Figure 3. The width of the impedance arc, the charge transfer resistance (R_{ct}), comprises the loss channels in the cell exclusive of the membrane ohmic resistance (R_Ω). We note that for two-electrode full-cell EIS such as is the case here, both electrodes in the cell contribute to R_{ct}, and control for that effect by using identical Pt-based cathodes for both cells. In the H_2-H_2 configuration, the Pt-Pt cell (Figure 4a) displays very small R_{ct} (0.06 Ω cm^2) that is insensitive to current, indicative of highly facile hydrogen oxidation/evolution kinetics. In contrast, R_{ct} in H_2-H_2 for the Ru-Pt cell is significantly larger, indicating that Ru indeed has a lower intrinsic activity for the HOR than Pt in the conditions studied. However, we note a significant departure from the room-temperature aqueous acid case in the relative magnitude of the activity of each[6]. From both the slope of the polarization curves in Figure 3 and the R_{ct} in Figure 4, we can estimate that Pt is more active than Ru by less than an order of magnitude in this case. This estimate is made under the low-field approximation, in which exchange current is inversely proportional to charge transfer resistance[24]. A more precise determination of relative activity is problematic, since in the case of solid acid systems an accepted gauge of electrochemical surface area has not yet been developed. The reasons for the differences in Ru activity are not yet known definitively, but we suggest that the low relative humidity at the operational temperature of 250 °C and 75 °C dew point (approximately 1% RH) results in a significantly modified adsorbate surface coverage compared to the aqueous case, promoting HOR reaction site availability.

In the CO-rich simulated reformate, R_{ct} for all of the cells is larger than in H_2 (Figure 4c,d). This is primarily a func-

tion of the presence of CO, which adsorbs on the catalysts and reduces the available sites for H_2 adsorption. A secondary effect results from the dilution of the H_2 stream (adding approximately 0.02 Ω cm^2 to R_{ct} in the case of Pt[2]). At OCV, R_{ct} for the Ru-Pt cell is comparable to that of the Pt-Pt cell. Far from the open circuit potential, however, the charge transfer impedance of the Pt-Pt cell increases more than 50%, while R_{ct} for the Ru-Pt cell remains identical. We attribute this disparity to the effective removal of CO from Ru, either via direct electrooxidation or the water-gas shift (WGS) reaction[25]; it is likely that both of these processes are occurring to some degree. In each scenario, CO is removed from the catalyst surface, yielding additional H_2 in the case of the WGS, and protons in the case of direct electrooxidation. These synergistic effects offset both the problems of CO site blockage and H_2 dilution in the reformate.

The hydrogen pump with the Ru-based anode showed excellent stability in the CO-rich reformate at a cell voltage of 0.1 V, as shown in Figure 5. After 160 hours, the cell displayed a net decline in performance of approximately 3 mA cm^{-2}.

Given the activity and stability of the Ru-based anodes in the hydrogen pump configuration, we sought to apply this concept to the anode of an electricity-generating fuel cell. The results of these tests are shown in Figure 6. In both pure hydrogen and in the CO-rich simulated reformate, the polarization curves of the cells with the experimental Ru anode and the control Pt anode are nearly identical. This is not surprising, since the differences in overpotential observed in hydrogen pump mode are small compared to the cathode overpotential, which is dominant in solid acid fuel cells and other proton-conducting fuel cell technologies.

4 Conclusions

We have demonstrated a remarkably simple method of synthesizing highly dispersed, carbon-supported nanometric Ru with very high metal loadings. We expect this method to prove similarly facile for synthesizing Ru-based anode catalysts for room temperature alkaline systems as well as other heterogeneous chemical reactions.

The materials synthesized are excellent and cost-effective hydrogen oxidation catalysts for electrochemical devices based on CsH_2PO_4, especially in CO-rich gas streams. The Ru-based electrocatalysts are able to effectively remove CO from their surface under high oxidation currents, while Pt catalysts show a marked decrease in performance under the same conditions.

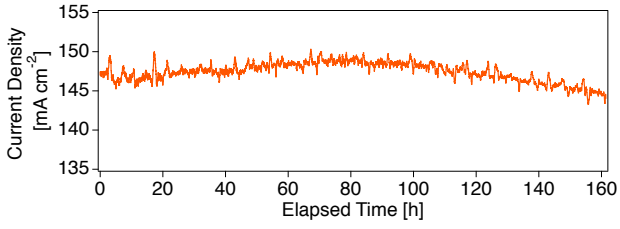

Fig. 5 Steady state hydrogen oxidation current for a Ru-based anode operating on simulated reformate at a 0.1 V cell overpotential.

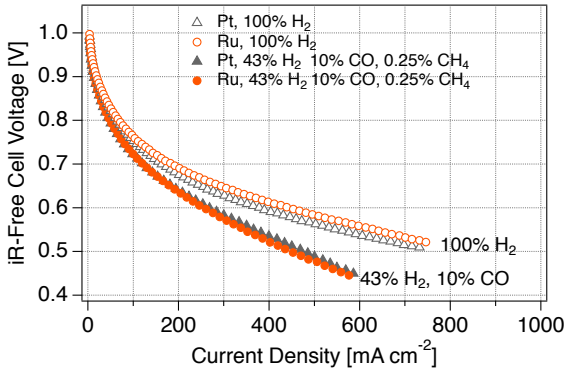

Fig. 6 iR_Ω-free polarization curves for solid acid fuel cells with Pt-based or Ru-based composite anodes acquired at 250 °C and 75 °C dew point in 100% H_2 and in a simulated reformate mixture. The full composition of the gas mixtures is detailed in the text. For each cell the cathode consisted of vapor-deposited Pt:CDP with a loading of 1.75 mg_{Pt} cm^{-2}

5 Acknowlegements

This work was supported by the Office of Naval Research (Award N000141210887). A portion of this research was conducted at the Center for Nanophase Materials Sciences, which is sponsored at Oak Ridge National Laboratory by the Scientific User Facilities Division, Office of Basic Energy Sciences, U.S. Department of Energy. A.B.P thanks Samuel St. John and Ramez Elgammal for helpful comments on the manuscript.

References

1 S. Haile, C. Chisholm, K. Sasaki, D. Boysen and T. Uda, *Faraday Discuss.*, 2007, **134**, 17.
2 A. B. Papandrew, D. L. Wilson, N. M. Cantillo, S. Hawks, R. W. Atkinson, G. A. Goenaga and T. A. Zawodzinski, *J. Electrochem. Soc.*, 2014, **161**, F679–F685.
3 A. B. Papandrew, C. R. I. Chisholm, R. A. Elgammal, M. M. Ozer and S. K. Zecevic, *Chem. Mater.*, 2011, **23**, 1659–1667.
4 H. Liu, C. Song, L. Zhang, J. Zhang, H. Wang and D. P. Wilkinson, *J. Power Sources*, 2006, **155**, 95–110.
5 S. Wasmus and A. Küver, *J. Electroanal. Chem.*, 1999, **461**, 14–31.
6 H. A. Gasteiger, N. M. Markovic and P. N. Ross, *J. Phys. Chem.*, 1995, **99**, 8290–8301.

7 J. Ohyama, T. Sato, Y. Yamamoto, S. Arai and A. Satsuma, *J. Am. Chem. Soc.*, 2013, **135**, 8016–21.

8 J. Ohyama, T. Sato and A. Satsuma, *J. Power Sources*, 2013, **225**, 311–315.

9 T. Hibino and K. Kobayashi, *J. Mater. Chem. A*, 2013, **1**, 7019.

10 J. M. Campelo, D. Luna, R. Luque, J. M. Marinas and A. a. Romero, *ChemSusChem*, 2009, **2**, 18–45.

11 J. Okal, *Catal. Commun.*, 2010, **11**, 508–512.

12 A. B. Papandrew, C. R. I. Chisholm, S. K. Zecevic, G. M. Veith and T. A. Zawodzinski, *J. Electrochem. Soc.*, 2012, **160**, F175–F182.

13 T. Aaltonen, *Mater. Res.*, 2005, 1–71.

14 T. Aaltonen, M. Ritala, K. Arstila, J. Keinonen and M. Leskelä, *Chem. Vap. Depos.*, 2004, **10**, 215–219.

15 M. Green, M. Gross and L. Papa, *J. Electrochem. Soc.*, 1985, **132**, 2677.

16 S.-F. Huang, Y. Chi, C.-S. Liu, a.J. Carty, K. Mast, C. Bock, B. MacDougall, S.-M. Peng and G.-H. Lee, *Chem. Vap. Depos.*, 2003, **9**, 157–161.

17 C. Vahlas, F. Juarez, R. Feurer, P. Serp and B. Caussat, *Chem. Vap. Depos.*, 2002, **8**, 127–144.

18 P. Serp, P. Kalck and R. Feurer, *Chem. Rev.*, 2002, **102**, 3085–128.

19 Y. Plyuto, I. Babich, L. Sharanda, A. de Wit and J. Mol, *Thermochim. Acta*, 1999, **335**, 87–91.

20 S. Musi, S. Popovi and A. Gajovi, *J. Mater. Sci. Lett.*, 2002, **21**, 1131 – 1134.

21 M. Lashdaf, T. Hatanpää, A. Krause, J. Lahtinen, M. Lindblad and M. Tiitta, *Appl. Catal. A Gen.*, 2003, **241**, 51–63.

22 J. W. Phair and S. P. S. Badwal, *Ionics (Kiel).*, 2006, **12**, 103–115.

23 K. A. Perry, G. A. Eisman and B. C. Benicewicz, *J. Power Sources*, 2008, **177**, 478–484.

24 A. J. Bard and L. R. Faulkner, *Electrochemical Methods: Fundamentals and Applications*, Wiley, 2nd edn, 2000.

25 T. Utaka, T. Okanishi, T. Takeguchi, R. Kikuchi and K. Eguchi, *Appl. Catal. A Gen.*, 2003, **245**, 343–351.